



## Research Article

## Evaluation of the influence of offshore wind farm noise on the fishes and dolphins in the Pearl River Estuary

Zhongchang Song<sup>a,\*</sup>, Weijie Fu<sup>a,1</sup>, Hongquan Li<sup>a,1</sup>, Yingnan Su<sup>a</sup>, Zhanyuan Gao<sup>a</sup>,  
Wenxin Fan<sup>b</sup>, Jiangang Hui<sup>a</sup>, Wenzhan Ou<sup>a,c</sup>, Shengyao Sun<sup>c,d</sup>, Teng Wang<sup>e</sup>,  
Honghui Huang<sup>e,\*\*</sup>, Yu Zhang<sup>a,\*\*\*</sup>

<sup>a</sup> Key Laboratory of Underwater Acoustic Communication and Marine Information Technology (Ministry of Education), College of Ocean and Earth Sciences, Xiamen University, Xiamen, 361005, China

<sup>b</sup> State Key Laboratory of Marine Environmental Science, College of the Environment and Ecology, Xiamen University, Xiamen, 361005, China

<sup>c</sup> State Key Laboratory of Marine Environmental Science, College of Ocean and Earth Sciences, Xiamen University, Xiamen, 361005, China

<sup>d</sup> Dongshan Swire Marine Station, Xiamen University, Dongshan, 363499, China

<sup>e</sup> Guangdong Provincial Key Laboratory of Fishery Ecology and Environment, South China Sea Fisheries Research Institute, Chinese Academy of Fishery Sciences, Guangzhou, 510300, China

## ARTICLE INFO

## Keywords:

Offshore wind farm  
Noise impact  
Propagation model  
Biological source  
Pile driving

## ABSTRACT

In this study, we recorded the noise radiating from a wind farm and evaluated its potential impact on the fishes and Indo-Pacific humpback dolphins (*Sousa chinensis*) residing in the Pearl River Estuary. The pile driving pulses, recorded 30 m from the construction site, had a mean zero-to-peak sound pressure level of 195.1 dB (re 1  $\mu$ Pa) ( $n = 238$ ), exceeding the hearing thresholds of both fishes and Indo-Pacific humpback dolphins. The operational noise from the wind farm was significantly lower in amplitude; therefore, our analysis primarily focused on the radiation of pile driving noise. Acoustic measurements taken at three different distances during pile driving events supported the development of an acoustic propagation model, which was then used to predict the sound exposure levels of pile driving pulses radiating from 5 m below the water surface. By referring to established noise exposure metrics, we estimated an impact zone of 12.8 m for fishes. For the Indo-Pacific humpback dolphins, the permanent and temporary threshold shift zones were predicted to be 32.4 m and 580.9 m, respectively. Our findings underscore the importance of increasing our understanding on hearing sensitivities of the local inhabitants in the Pearl River Estuary and identify their core habitats. This approach enabled us to use the model to estimate impact zones and better protect the local marine life from the effects of pile driving noise radiation.

## 1. Introduction

The use of fossil fuels has led to significant issues such as global warming, affecting both land and ocean environments (Burrows et al., 2011; Doney et al., 2012; Hoegh-Guldberg et al., 2019; Arneth et al., 2020). This has created a growing need for clean and affordable energy sources to reduce greenhouse gas emissions (U.S. Energy Information Administration, 2019; Umar et al., 2021). Offshore wind energy, as a form of blue energy, presents a promising solution (Bailey et al., 2014; Gielen et al., 2019) and has been generating commercial electricity since

2002 (Breton and Moe, 2009; Corbetta et al., 2014). The share of electricity generated by offshore wind farms is projected to reach 1000 GW by 2050 (Global Wind Energy Council, 2020; IRENA, 2020). The coming years will likely witness a substantial expansion of offshore wind farms (Deng et al., 2022), and the associated infrastructure and operations will inevitably impact local ecosystems (Koschinski et al., 2003; Cook et al., 2018; Niu et al., 2023). There are still significant gaps in scientific knowledge regarding the ecological impacts of wind turbines during both construction and operation, which need to be addressed through further research.

\* Corresponding author.

\*\* Corresponding author.

\*\*\* Corresponding author.

E-mail addresses: [songzc@xmu.edu.cn](mailto:songzc@xmu.edu.cn) (Z. Song), [huanghh@scsfri.ac.cn](mailto:huanghh@scsfri.ac.cn) (H. Huang), [yuzhang@xmu.edu.cn](mailto:yuzhang@xmu.edu.cn) (Y. Zhang).

<sup>1</sup> These authors contributed equally to this paper.

Most existing studies addressing the impact of wind farms on animals focus on marine mammals, birds, and fishes (Hall et al., 2020). Pile driving releases strong acoustic energy into both the substrate and water, disrupting the natural habitats of local fauna and affecting the presence of biota. After construction, turbine towers provide additional shelter for benthic organisms and resting areas for birds (Wilson et al., 2010; Furness et al., 2012; Vanermen et al., 2015; Causon and Gill, 2018). This may increase biomass and biodiversity and increase food availability for top predators like odontocetes (Wilhelmsson et al., 2006; Langhamer et al., 2018). Scheidat et al. (2011) found that after construction, harbor porpoises (*Phocoena phocoena*) showed resilience to the operation of wind turbines, with increased occurrences within the wind farm area. However, they cautioned that these conclusions might be specific to that case and should not be uncritically generalized to other wind farms. In most studies, the noise produced during construction and long-term operation exerts pressure on animals, potentially masking their communication and reducing their fitness (Debusschere et al., 2016; Neo et al., 2016; Stanley et al., 2017).

Many marine animals, including odontocetes, fishes, squid, snapping shrimp, and lobsters can hear sounds underwater and use acoustic cues to navigate their environment (Nachtigall and Supin, 2008; Mooney et al., 2010; Hughes et al., 2014; Popper et al., 2019; Dinh and Radford, 2021; Jézéquel et al., 2021). The hearing sensitivities of fish and marine invertebrates are generally confined to frequencies below 1000 Hz, which overlaps with the spectrum of pile-driving pulses (Jones et al., 2021; Cones et al., 2022; Niu et al., 2023). Although odontocetes have their best hearing sensitivity in the high-frequency range, they can still be affected by the intense noise from pile driving. Branstetter et al. (2018) reported a significant reduction in target detection performance in bottlenose dolphins (*Tursiops truncatus*) when exposed to pile-driving noise at 140 dB (re 1  $\mu$ Pa), which exceeded their hearing thresholds at 2 kHz (Accomando et al., 2020). The impact of such noise can extend over a considerable distance due to its slow attenuation at low frequencies. For instance, the sound exposure level of a pile-driving pulse was measured at 140.1 dB (re 1  $\mu$ Pa<sup>2</sup>s) even at 4573 m from the construction site, causing injuries to local aquaculture fish (Niu et al., 2023). Additionally, the intervals between echolocation events in harbor porpoises increased after pile driving, with this effect observed at distances exceeding 20 km (Carstensen et al., 2006; Tougaard et al., 2009). For bottlenose dolphins, disturbances may occur up to 50 km away (Bailey et al., 2010).

This raises an important issue regarding the evaluation and mitigation of the impact of pile-driving events during construction. Reducing the radiated energy of pile-driving noise is crucial to minimizing its impact on marine life. One effective mitigation method involves the use of bubble structures, which have been employed to protect harbor porpoises (Lucke et al., 2011). A bubble curtain is created by placing a perforated hose on the seabed and pumping air into it at the construction site. For large monopiles, a double bubble curtain system can create a stronger noise barrier, further reducing the radiated energy (Koschinski and Lüdemann, 2020). In some cases, sound barriers are fabricated by using gas-filled elastic balloons or robust foam (Elmer, 2018). However, the range of influence from pile-driving events at different sites remains to be thoroughly investigated, even with the use of these bubble mitigation techniques.

In this paper, we evaluated the impact of pile-driving noise on the animals inhabiting the Pearl River Estuary, which includes a natural reserve area for Indo-Pacific humpback dolphins (*Sousa chinensis*). This wind farm is in one of several sites along the Chinese coastline selected by the government to supply long-term electricity (Guangdong Provincial Development and Reform Commission, 2018; Tu et al., 2021; Lian et al., 2022). The estuary is home to a diverse range of aquatic animals (Huang et al., 2012; Wang et al., 2017, 2022; Song et al., 2023b), and it is crucial to address the potential impact of wind farm noise on these species to inform management practices that can mitigate such effects. This study, guided by criteria outlined in the technical report by the National Marine Fisheries Service (2018), investigates the impact of operational noise on

fishes and Indo-Pacific humpback dolphins.

## 2. Materials and methods

### 2.1. Acoustic recording and analysis on animal sounds at the wind farm

We used an offshore wind farm located in the eastern part of the Pearl River Estuary (PRE) (Fig. 1A). The PRE is characterized by high biodiversity, including dolphins, finless porpoises, crustaceans, fishes, and benthic animals (Huang et al., 2002; Zhang et al., 2017; Cheang et al., 2020; Kuang et al., 2021), with many of these inhabitants capable of producing sounds (Fig. 1B). The wind power plant comprises over 30 wind turbine generators, covering a total area of more than 30 km<sup>2</sup>. Each turbine has a diameter of 8.25 m, a length of 84 m, a weight of 1200 tons, and a power output of 3 MW. The northern part of the plant area is located 4.9 km away from the natural reserve of Indo-Pacific humpback dolphins in the PRE.

Sounds produced by Indo-Pacific humpback dolphins and fishes were recorded during a field survey conducted in August 2021 using a compact recording system, the SoundTrap recorder (ST 300 HF, Ocean Instruments Ltd, New Zealand). The recorder featured a linear frequency range of 20 Hz–150 kHz ( $\pm 3$  dB), with a sensitivity of -188.7 dB (re 1 V/ $\mu$ Pa) in low gain mode and a sampling rate ranging from 48 kHz to 576 kHz. The internal noise level was less than 37 dB (re 1  $\mu$ Pa) above 2 kHz, and the data were saved in .wav files. Although the PRE is one of the critical habitats for Indo-Pacific humpback dolphins in China, encounters with the dolphins were somewhat opportunistic during our survey.

Our survey, titled “2021 OCEAN-HK (TRS) Cruise Plan”, took place from August 26 to September 2, 2021, with the primary aim of collecting water samples and background noise. We encountered dolphins on several occasions, but since the vessel was cruising during most of these encounters, deploying the recorder was challenging. However, on August 29, 2021, while the vessel was anchored for a 4-h duty cycle at a specific location (22.080° N, 113.592° E), we encountered the dolphins again. This time, we successfully deployed the SoundTrap recorder, capturing dolphin clicks with a sampling rate of 576 kHz. At each duty location, which typically lasted 4–5 h, the acoustic recorder was suspended 1.5 m below the water surface to collect sounds.

The dolphin clicks were analyzed using customized MATLAB codes. A Butterworth high-pass filter with a cutoff frequency of 5 kHz was applied to filter out low-frequency noise, such as seawater fluctuations. To extract individual clicks from the click trains, the trains were transformed into the time-frequency domain using the following formulas:

$$F(f, m) = STFT\{x[n]\}(m, f) = \sum_{n=0}^N x[n]\omega[n - m]e^{-j2\pi fn} \quad (1)$$

$$P(f, m) = 10 \log_{10}(\text{abs}(F(f, m))) \quad (2)$$

In this analysis,  $F(f, m)$  represents the short-time Fourier transform (STFT) of the click signal  $x[n]$ , calculated using a 1024-point fast Fourier transform with a 43.5% overlap and a Hann window (Yang et al., 2017; Song et al., 2023a). To isolate the clicks from the surrounding background noise, a pixel threshold was applied to the spectrogram, setting values below the threshold to zero. This allowed for the precise determination of the time location of each click for extraction.

The PRE is also recognized as a site rich in fish diversity, with recent reports confirming a high abundance of fish in the offshore wind farm area (Wang et al., 2022). However, fish calls can be easily masked by background noise, especially after long-range propagation. To address this, we manually examined the fish calls and compared them to those produced by the Chinese bahaba (*Bahaba taipingensis*) recorded at a local fish aquaculture facility (Li et al., 2023). Both dolphin clicks and fish calls were manually reviewed to ensure the collection of clean, high-quality acoustic datasets for subsequent analysis.

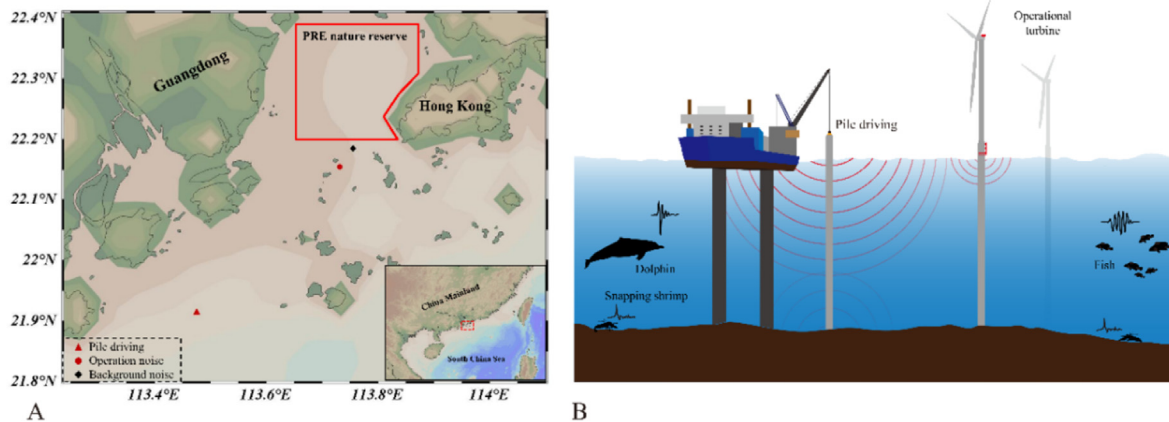


**Fig. 1.** (A) Location of the offshore wind farm recording sites in the Pearl River Estuary for normal operation measurement in Guishan waters (red circle) and pile driving events in Jinwan waters (red triangle). (B) An illustration of the biodiversity in the wind farm region, with three marine taxa that can both produce and sense sounds: snapping shrimp, fishes, and Indo-Pacific humpback dolphins.

**2.2. Acoustic recording of the operation and pile driving noise**

Measurements of the operational noise were conducted within the wind farm, where the first set of 31 turbines was running in Guishan waters (south of the PRE) on April 18, 2019 (Fig. 2). These turbines represent the majority of the wind farm facilities constructed during the first phase from 2016 to 2019. Upon arrival at the site, we anchored the vessel and turned off the engine to eliminate any noise interference from the vessel. The distance between the turbine and the vessel was estimated. A hydrophone (RHSA10, Applied Acoustics Research Institute, Hangzhou, China) with a linear working frequency of 20 Hz–200 kHz ( $\pm 3$  dB), a sensitivity of  $-185$  dB (re  $1$  V/ $\mu$ Pa), and a preamplifier of 26 dB was used for the recordings. The recordings were transmitted to a computer via a DAQ Card (6216, National Instruments, USA) for storage, with the sampling rate set at 240 kHz.

On April 18, 2019, we deployed the hydrophone 3 m underwater and measured the noise produced by a specific turbine. The measurement was

conducted 20 m from the turbine foundation in water with a depth of 8 m. Recording began at 0900 and lasted approximately 10 min under Beaufort sea state level 2, with a wind speed of 5.28 m/s. The noise data were segmented into 10-s intervals, and the mean power spectral density was calculated for each segment. For comparison, background noise was measured 4.9 km away from the wind farm, ensuring it was free from operational noise. These background recordings were also segmented into 10-s intervals for parallel analysis.

The pile-driving noise was measured within the wind farm on January 17, 2020, in Jinwan waters, west of the PRE. A microMARS recorder (Desert Star System, Marina, CA, USA) with a sensitivity of  $-177$  dB (re  $1$  V/ $\mu$ Pa) was deployed 3 m underwater, where the water depth was 14.8 m. Noise measurements were taken at distances of 30, 60, and 90 m from the pile-driving site. The recordings began at 1400 and, at each location, lasted approximately 30 min, capturing one pile-driving session per location. The sampling rate was set at 64 kHz. During the recording period, the Beaufort sea state level ranged from 2 to 3, with

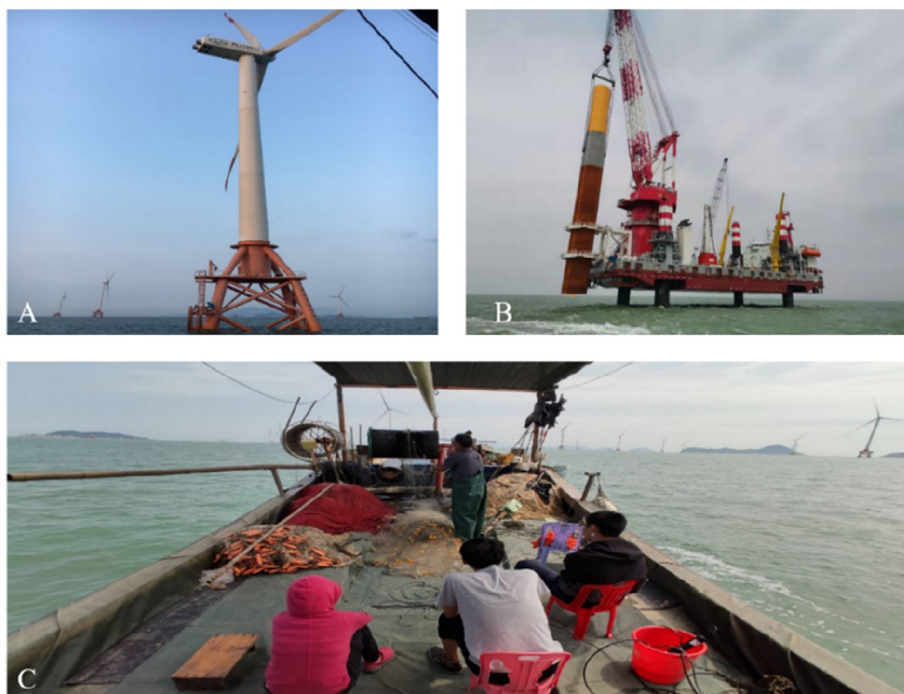


**Fig. 2.** (A) The recording site of a wind farm turbine in Guishan waters, Pearl River Estuary. (B) The pile driving site during the construction of the offshore wind farm in Jinwan waters, Pearl River Estuary. (C) The recording vessel.

wind speeds between 5.6 m/s and 6.2 m/s.

The construction produced periodic pulses, and we initially manually examined the recorded files before using customized MATLAB (Math-Works, Cambridge, MA) codes to extract the pile-driving pulses from the background noise. Each pulse had a duration of approximately 400 ms. Background noise was measured after the pile-driving events had ceased and was segmented into 400 ms pieces for comparative analysis.

### 2.3. Estimation of pile-driving pulse radiation

To assess the impact of pile-driving noise, we estimated the acoustic radiation field by developing a propagation model. The model used a water layer depth of 11 m (Fig. 3), with an omnidirectional point sound source placed at a depth of 5 m to initiate sound propagation at various frequencies. The water density was set at 1.024 g/cm<sup>3</sup>, and the sound speed profile, derived from previous measurements, ranged from 1531.4 m/s at the sea surface to 1536.9 m/s at the sea bottom. The silty sand sediment layer was characterized by a density of 1.83 g/cm<sup>3</sup>, a sound speed of 1677 m/s, and an attenuation coefficient of 0.75 dB/λ.

Pile driving generates Mach waves in the water (Reinhall and Dahl, 2011; Song et al., 2023c). However, the dynamic nature of this process cannot be fully incorporated into the propagation model. As a simplification, we used a point sound source and employed a parabolic propagation model to predict the acoustic fields of the pile-driving noise. The horizontal resolution was set at 0.1 m, while the vertical resolution varied with frequency to ensure at least six samples per wavelength.

### 2.4. Estimation of pile driving noise impact zone on fish

The hearing sensitivities of red drum (*Sciaenops ocellatus*), a species inhabiting the PRE, range between 100 and 1200 Hz (Horodysky et al., 2008). Consequently, we calculated the transmission loss (TL) field of the pile-driving pulse noise within this frequency range. The range was divided into 100-Hz width bands, resulting in a total of 12 bands. The center frequency of each band was used to model the TL for that specific band.

We incorporated our acoustic analysis of the pile-driving noise with the weights at each center frequency determined by the spectral distributions. Given that the pile-driving noise was measured at a distance of 30 m from the construction site, we estimated the source level for each frequency band at 1 m from the sound source using the following method:

$$SL_i = 10 \log_{10} \left( \int_{f_{Li}}^{f_{Hi}} S(f) df \right) + TL_i(r_0, d_0) \quad (3)$$

where  $SL_i$  and  $TL_i$  are the source level and  $TL$  distribution of the  $i_{th}$  frequency band in dB, with  $f_{Hi}$  and  $f_{Li}$  as the upper and lower frequencies respectively.  $S(f)$  is the power spectrum density. The overall sound pressure level (PL) at each frequency band was calculated using:

$$PL_i = SL_i - TL_i \quad (4)$$

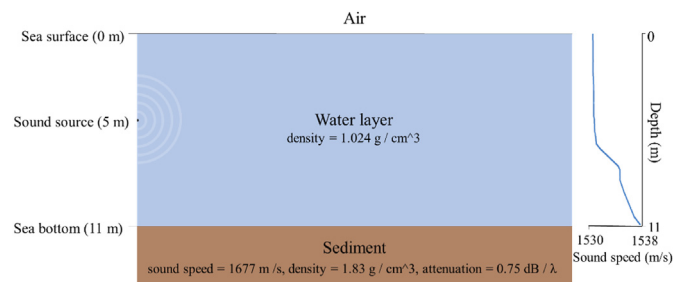


Fig. 3. Settings of the sound propagation model.

And then we calculated:

$$SEL_{ss} = 10 \log_{10} \left( t \cdot \sum_{i=0}^{i=N} 10^{(PL_i)/10} \right) \quad (5)$$

where  $SEL_{ss}$  represents the sound exposure level of a single pile driving strike.

To evaluate the impact of pile-driving exposure over time, the cumulative sound exposure level ( $SEL_{cum}$ ) field was calculated by integrating the squared sound pressure  $P(t)$  over period  $T$  (Martin et al., 2019):

$$SEL_{cum} = 10 \log_{10} \left( \frac{1}{T_0 p_0^2} \int_0^T P(t)^2 dt \right) \text{ dB re } 1 \mu\text{Pa}^2 \cdot \text{s} \quad (6)$$

where  $T_0$  and  $p_0$  are set as 1 s, and 1 μPa, and  $T$  is the signal duration. We recorded 636 pile pulses at 30 m, with each pulse lasting 0.4 s and with the pulse interval approximately 1.0 s.

$SEL_{cum}$  can also be estimated using the formula from Halvorsen et al. (2011):

$$SEL_{cum} = SEL_{ss} + 10 \log 10(N) \quad (7)$$

where  $N$  represents the total number of the pulses that are produced throughout the period.

The biological impact of pile driving sounds on fishes was related to both  $SEL_{cum}$  and the number of strikes, which can be described according to Halvorsen et al. (2011, 2012) as:

$$\ln(RWI + 1) = 0.149 \times SEL_{cum} - 30.050 - 0.000171 \times N \quad (8)$$

According to equation (7), equation (8) can be converted as follows:

$$\ln(RWI + 1) = 0.149 \times (SEL_{ss} + 10 \log 10(N)) - 30.050 - 0.000171 \times N \quad (9)$$

where  $RWI$  is the response weighted index, defined as:

$$RWI = \sum_i^m (W_i \times T_i) \quad (10)$$

where  $i$ , and  $m$  represent the injury type index and number of injury types, respectively (Halvorsen et al., 2011, 2012).  $W_i$  is the trauma category weight that corresponds to injury type  $i$ . Injury types were defined as mortal, moderate, and mild, with respective  $W_i$  values of 5, 3, or 1. The proportion of the sample of fish exposed to a treatment that experienced injury type  $i$  determines  $T_i$ .

In equation (9),  $RWI$  is merely dependent on  $SEL_{ss}$  and the number of strikes  $N$ . To determine the weight for each injury type, we used previously published data on exposure experiments conducted on fish. Halvorsen et al. (2011, 2012) determined an  $RWI$  of 2 was the acceptable threshold for juvenile Chinook salmon (*Oncorhynchus tshawytscha*) under which no life-threatening effects were induced from 1 or 2 mild injuries. Using this, we then calculated a safety threshold of  $SEL_{ss}$  for fish under a strike number of 636, which was 181.74 dB (re 1 μPa<sup>2</sup>·s). This value was further used to estimate the impact zone for fish by emphasizing the zones with  $SEL_{ss}$  values over 181.74 dB (re 1 μPa<sup>2</sup>·s).

To evaluate the accuracy of the model, we used the data recorded from 30, 60, and 90 m away from the pile driving site. The modeled sound exposure level at these distances were compared to field measurements.

### 2.5. Estimation of the pile driving noise impact zone on dolphins

$SEL_{cum}$  is an important indicator for evaluating the impact of anthropogenic noise on odontocetes as well. To do this, the noise power spectrum was split into several 1/3 octave bands (National Marine Fisheries Service, 2018; Martin et al., 2019; Tougaard and Beedholm,

2019; Southall et al., 2019). The sound pressure fields of all the bands were weighted by an auditory weighting function  $W_{aud}(f)$  given by the National Marine Fisheries Service (2018), to emphasize the frequencies where the dolphins are sensitive and de-emphasize the frequencies where the animals are insensitive. The equation is expressed here in linear units of power:

$$W_{aud}(f) = 10^{C/10} \cdot \frac{(f/f_1)^{2a}}{[1 + (f/f_1)^2]^a [1 + (f/f_2)^2]^b} \quad (11)$$

where  $f$  is the frequency in Hz,  $C$  is the gain parameter in dB,  $f_1$  and  $f_2$  are cut off frequencies in Hz, and  $a$  and  $b$  are frequency exponents. These parameters vary with the marine mammal hearing group. For the Indo-Pacific humpback dolphin, the values of  $C$ ,  $a$ ,  $b$ ,  $f_1$ , and  $f_2$  are 1.2 dB (re 1  $\mu$ Pa), 1.6, 2, 8800 Hz, and 110,000 Hz, respectively (Southall et al., 2019; Martin et al., 2019). To reflect the overall noise exposure impact on these dolphins, the weighted sound pressure of all the bands were then integrated to get the weighted sound exposure level (Martin et al., 2019):

$$SEL_{w\_cum} = 10 \log_{10} \left( \frac{\int_0^{f_s/2} W_{aud}(f) S(f) df}{T_0 P_{ref}^2} \right) \quad (12)$$

where  $f_s$  is the sampling rate in Hz,  $S(f)$  is the power spectrum density,  $T_0$  is the reference time of 1 s, and  $P_{ref}$  is the reference pressure for 1  $\mu$ Pa. The temporary threshold shift (TTS) represents changes in hearing sensitivity that can recover over time, while the permanent threshold shift (PTS) describes a permanent loss in hearing. Indo-Pacific humpback dolphins belong to the high-frequency cetaceans (Martin et al., 2019), and the  $SEL_{w\_cum}$  thresholds of the TTS and PTS under the impulsive noise radiation are 170 and 185 dB, respectively (Southall et al., 2019). We used these values to estimate the TTS and PTS zones.

### 3. Results

#### 3.1. Biological acoustics

The fishes and dolphins produced signals (Fig. 4A, B and 4C). A total of 18 fish calls and 375 dolphin clicks were recorded. No whistles were

captured during the recording in the PRE, so we used 10 whistles recorded from another reserve for Indo-Pacific humpback dolphins (Zhang et al., 2024).

An example fish call exhibited oscillations of three cycles, with most of the energy confined below 2 kHz (Fig. 4D). Fish calls peaked at 562.5 Hz with a power spectral density of 103.5 dB (re 1  $\mu$ Pa), which dropped by 10 dB at 1.6 kHz. An example dolphin click demonstrated its short duration and broadband characteristics (Fig. 4C). The click waveform showed several oscillations, with a peak frequency of 84.9 kHz and a spectral density of 87.4 dB (1  $\mu$ Pa<sup>2</sup>/Hz). The -10 dB bandwidth was 114.4 kHz, ranging from 27.3 kHz to 141.7 kHz. Whistles, which have a longer duration than clicks, overlapped with background noise above 4 kHz. Ambient noise was higher between 250 Hz and 1 kHz, decreasing above 1.2 kHz.

Overall, the biological soundscape in the PRE covered a broad range. These data hold great value to examine the influence of wind farm noise on animals.

#### 3.2. Acoustics of wind farm noise

The spectrogram and time series of the operation noise showed a higher amplitude than the background noise below 2.5 kHz (Fig. 5), with a distinct peak at 281.3 Hz. It was difficult to find any pattern either in the spectrogram or the time domain (Fig. 5A and B).

The pile driving pulse showed a sharp amplitude onset and a gradient decrease (Fig. 6), with amplitude consistently higher than the background noise. The majority of the energy was confined between 77.6 and 217.2 Hz, with a power spectral density level of 158.7 dB (1  $\mu$ Pa<sup>2</sup>/Hz) at its peak frequency (155.0 Hz).

The pile driving pulse recorded 30 m away from the construction site was much stronger than the signals produced by the animals and their hearing thresholds (Fig. 7). These analyses demonstrated that if the animals were at the same spot where the noise was measured, their conspecific detection and communication ranges would have been reduced due to pile driving sounds. As the operation noise was lower than the hearing thresholds of the animals, we focused on addressing the impact zone of pile driving pulses.

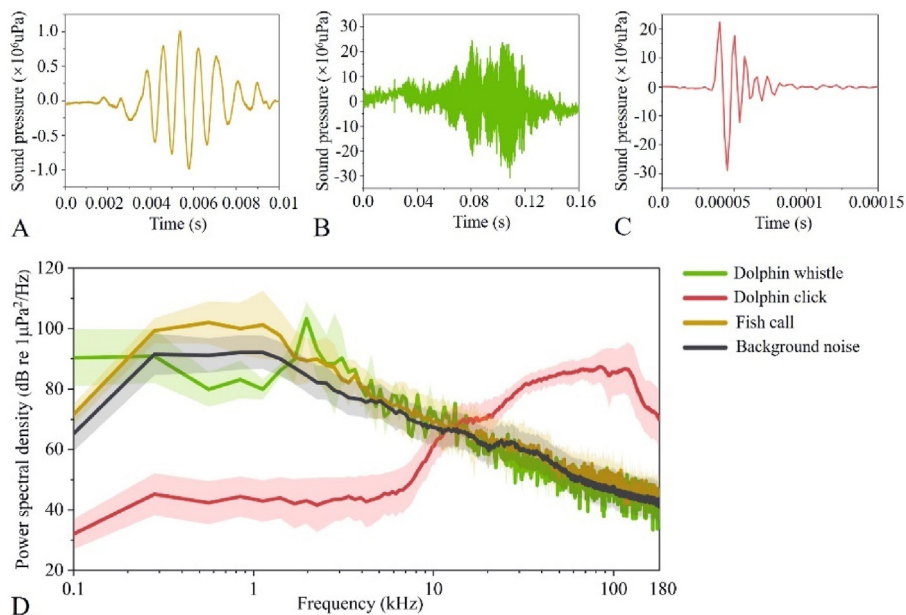
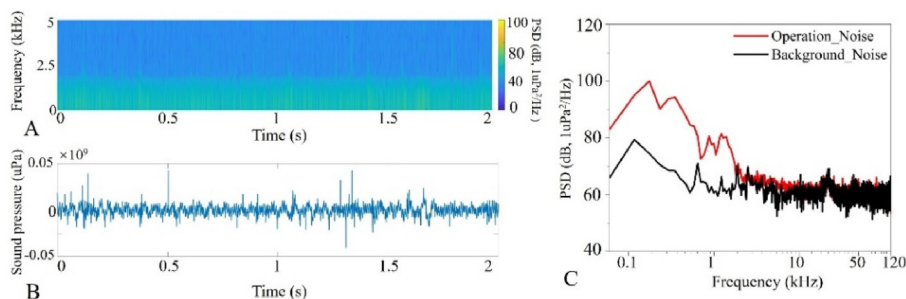
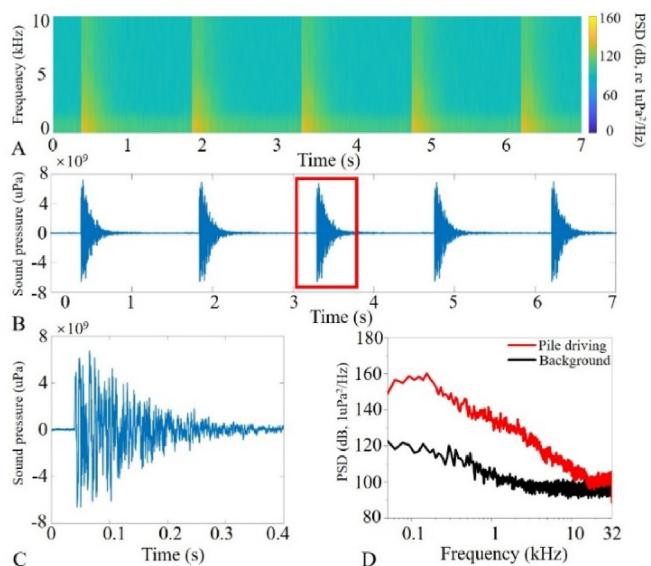


Fig. 4. The example waveforms of (A) a fish call, and (B) a whistle and (C) a click of an Indo-Pacific humpback dolphin. (D) The mean power spectral densities of the ambient noise, dolphin whistles, fish calls, and dolphin clicks, where the shadows depict the standard deviations.



**Fig. 5.** Acoustic characteristics of the noise produced during the operation phase at Guishan waters in the Pearl River Estuary. The operation noise is illustrated in (A) the time-frequency domain and (B) time domain. (C) The mean power spectral densities (PSD) of operation noise ( $N = 11$ ) and background noise.



**Fig. 6.** Acoustic characteristics of the pile driving signal recorded at the wind farm located at Jinwan waters in the Pearl River Estuary, approximately 30 m from the construction site. (A) Spectrogram of impact driving events illustrating time-frequency domain. (B) The waveform of the pile driving events. (C) The illustration of a specific pile driving pulse. (D) The mean power spectral densities (PSD) of pile driving pulses ( $n = 81$ ) and background noise.

### 3.3. The radiation field of pile driving noise and its impact zone

The transmission loss, sound pressure level, and sound exposure level fields we estimated did not simply follow a monotonic decrease. Generally, we found an attenuation with distance but this was accompanied by local increases (Fig. 8).

We used our field data recorded at 30, 60, and 90 m away from the pile driving site to validate the modelling results by comparing the mean  $SEL_{ss}$  of the pile driving pulses at each distance to the value estimated by the model (Fig. 8C). We found differences of 1.56, 2.65, and 1.01 dB between the field data and modeling at 30, 60, and 90 m respectively (Table 1), resulting in an average error of 1.74 dB, lower than those in previous studies (Han and Choi, 2022; Xie et al., 2024) thus verifying our model.

The  $SEL_{ss}$  field in Fig. 8C was recalculated for the frequency range between 100 Hz and 1200 Hz, where fish are most sensitive.  $SEL_{ss}$  values below the exposure threshold of 181.74 dB were set to null, creating the blank areas seen in Fig. 9.  $SEL_{ss}$  values exceeding this threshold were used to estimate the impact zone for fish. The pile driving was found to have an impact range of 12.8 m for fish (Fig. 9).

The propagation modes were complex, and the amplitude of the  $SEL_{ss}$  did not follow a simple monotonic decrease with increasing distance

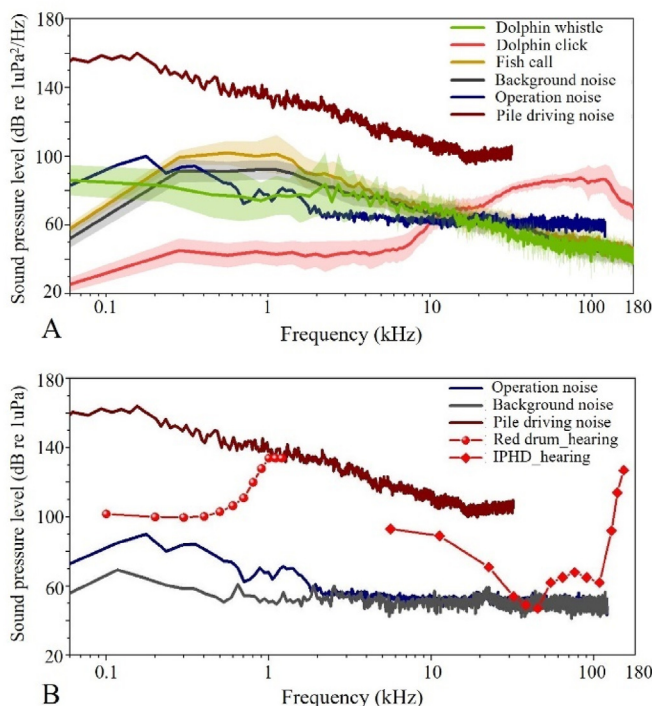


**Fig. 7.** (A) The mean power spectral densities of dolphin whistles ( $n = 10$ ) and clicks ( $n = 375$ ), fish calls ( $n = 18$ ), pile driving pulses ( $n = 81$ ), operation noise ( $n = 11$ ), and background noise. (B) The comparison between the noise (pile driving pulse, operation noise, and background noise) and the hearing thresholds of red drum (Horodysky et al., 2008) and IPHD (Indo-Pacific humpback dolphins, Li et al., 2012).

from the source, even at different depths. Salas et al. (2022) demonstrated that at specific frequencies, deeper waveguides support more propagating modes. As the number of modes increases, wave propagation becomes more complex, and the superposition of these modes results in non-spherical or non-cylindrical spreading. The safety range at each water depth was defined as the farthest point where the  $SEL_{ss}$  exceeded 181.74 dB (re  $1 \mu Pa^2 s$ ). Consequently, the null space representing the safe region was not uniform across different depths. The maximum impact range was estimated to be 12.8 m at a depth of 2.5 m.

### 3.4. Estimation of impact zone on dolphins

We referred to the criteria of the permanent and temporary hearing threshold shifts to estimate the respective PTS and TTS zones (Southall et al., 2019). The sound exposure level was calculated up to 8000 m (Fig. 10). The PTS impact zone covered a range of 32.4 m while the TTS zone was predicted as 580.9 m at a water depth of 2.65 m.

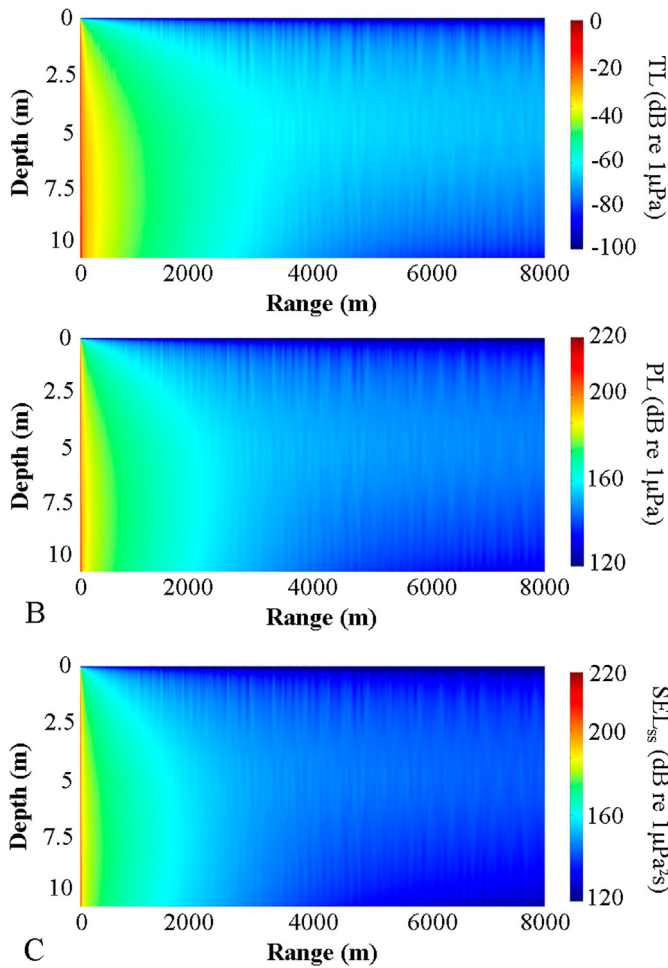


**Fig. 8.** (A) Predicted transmission loss (TL). The predicted (B) sound pressure level (PL) and (C) sound exposure level (SEL) fields for a single pile driving pulse. These fields were incorporated from 100 Hz to 32,000 Hz.

**Table 1**

Validation of the propagation model.

Distance/ m	Depth /m	Mean $SEL_{ss}$ (Field Measurement) /dB re 1 $\mu Pa^2 \cdot s$	$SEL_{ss}$ (Model) /dB re 1 $\mu Pa^2 \cdot s$	Error /dB	Percentage Error
30	3	176.36	177.92	1.56	0.88%
60	3	176.14	178.79	2.65	1.50 %
90	3	174.60	175.61	1.01	0.58%

**4. Discussion**

Although pile-driving noise is identified as the main threat in this study, it is important to note that, over time, the cumulative operational noise could reach a  $SEL_{cum}$  high enough to impact animals, especially at

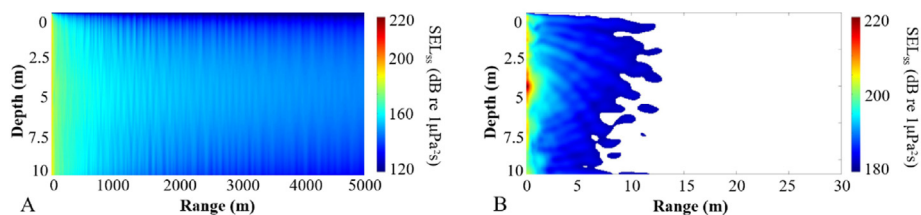


**Fig. 9.** (A) The predicted sound exposure level (SEL) field of a single pile driving pulse. These fields were predicted in a broadband scale, which was incorporated from 100 Hz to 1200 Hz. (B) The predicted impact zone of pile driving for fish, where the  $SEL_{ss}$  values are higher than the fish safety threshold of 181.74 dB.

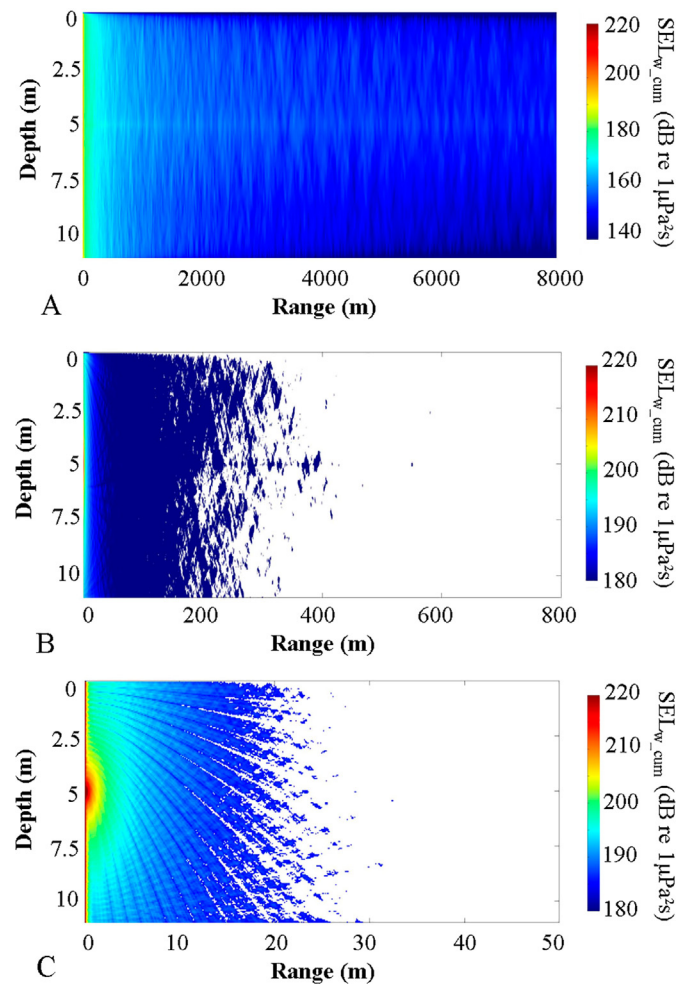


**Fig. 10.** (A) The predicted weighted sound exposure level ( $SEL_{w,cum}$ ) field of the pile driving pulse from a source at a depth of 5 m. Estimated (B) temporary and (C) permanent threshold shift zones using 170 and 185 dB as criteria respectively (Southall et al., 2019).

close ranges. For instance, if a fish was located at the same site as the hydrophone, the operational noise measured 20 m from the turbine was higher than fish calls below 300 Hz (Fig. 7A). It is reasonable to extrapolate that at closer distances, operational noise may mask an animal's vocalizations and hearing, particularly for species sensitive to low-frequency sounds below 1.5 kHz. Although the exact locations where animals produce or hear sounds are unknown, it is possible that operational noise could mask fish vocalizations below 200 Hz within 20 m of the turbine (Fig. 7A). At close ranges, this noise may mask fish communication, leading to negative effects (de Jong et al., 2020; Zhang et al., 2021; Siddagangaiah et al., 2022).

The current study was based on recordings from a single operating turbine, but there are dozens of turbines in the Guishan waters wind

farm. The cumulative contribution from multiple turbines could create a larger impact zone and exert a considerable effect on local aquatic animals, which cannot be ignored (Tougaard et al., 2020).

In comparison, pile-driving noise significantly masks animal's vocalizations and hearing if they are within the range where acoustic measurements were taken (Fig. 7A and B), and this masking effect could extend over long distances. Niu et al. (2023) reported a peak-to-peak sound pressure level of 170.9 dB (re 1  $\mu\text{Pa}$ ) at 3563 m from the pile-driving site, where large yellow croaker (*Pseudosciaena crocea*) exhibited acute behavioral responses to the noise. The disturbance caused by pile-driving noise can extend up to 50 km for bottlenose dolphins and 20 km for harbor porpoises from the construction site (Bailey et al., 2010; Tougaard et al., 2009). The response distance may vary among species due to differences in hearing and environmental factors (Ellison et al., 2012). Collecting baseline information is crucial for developing appropriate noise exposure criteria for marine mammals (Southall et al., 2008; Leunissen et al., 2019).

It is important to note that the formula  $SEL_{cum} = SEL_{ss} + 10\log_{10}(N)$  is applicable when the sound exposure level of a single pulse exceeds the threshold that induces hearing or physical impacts in animals (Halvorsen et al., 2011). Halvorsen et al. (2011) highlighted the insufficiency of using a single metric,  $SEL_{cum}$ , to determine noise impact.  $SEL_{ss}$  and the total number of strikes remain critical parameters in evaluating overall noise exposure. If the  $SEL_{ss}$  of any noise type is below the impact threshold, continuous noise accumulation would not lead to detrimental effects on animals. In our study, the pile-driving pulse had a mean  $SEL_{ss}$  of 176.4 dB (re 1  $\mu\text{Pa}^2\text{s}$ ) at 30 m from the construction site, while the model estimated the  $SEL_{ss}$  at 0.1 m could be as high as 219.3 dB (re 1  $\mu\text{Pa}^2\text{s}$ ). Therefore, the  $SEL_{ss}$  of the pile-driving pulse is strong enough to impact fish at close range. Using the biological response metric, *RWI*, derived by Halvorsen et al. (2011, 2012), and an *RWI* of 2, we estimated a maximum impact range of 12.8 m for fish. Considering that pile-driving events may occur simultaneously in the wind farm during construction, the spatial superposition of these noises could result in a large area of impact.

The spatial distribution of acoustic fields was estimated under several assumptions, including the source location. Since the acoustic field varies with the depth of the source and frequency (Oliveira et al., 2021; Salas et al., 2022; Zhou et al., 2022), the impact areas would differ if we applied the same lethal, injury, and TTS criteria to acoustic fields estimated with sources at different depths. This study simplified the model by using a point sound source at a specific water depth, as the dynamic process of pile driving and Mach waves were not incorporated into the propagation simulation (Reinhal and Dahl, 2011; Song et al., 2023c). In the future, this issue could be addressed by setting a series of sound sources at different depths with respective amplitude weights. The resulting fields could then be combined into an overall field to estimate lethal, injury, and TTS impact zones.

Although we did not measure the particle motion component of the pile-driving and operational noise, it is likely that the noise interferes with the detection of particle motion by fish and invertebrates (Ladich and Fay, 2013; Popper and Hawkins, 2018). Sigray et al. (2022) reported a strong zero-to-peak particle acceleration of up to 129 dB (re 1  $\mu\text{m}/\text{s}^2$ ) at 580 m from the piling operation site. If animals such as fish, squid, and snapping shrimp are exposed to strong particle motion stimuli, it may lead to physiological and behavioral changes (Jones et al., 2021; Davidsen et al., 2019). Extending findings from previous studies to the PRE region (Hawkins and Popper, 2017; Popper et al., 2022) suggests that wind farm noise could interfere with animals through strong particle motion inputs. Much more research is needed to address particle motion from wind farm activities.

The TTS zone for Indo-Pacific humpback dolphins in the PRE was estimated to be 580.9 m, comparable to the 500-m safety zone proposed by Wang et al. (2014). The pile-driving pulses in this study had a much higher  $SEL_{w,cum}$  than vibratory pile sounds reported by Wang et al. (2014). The duration used to calculate  $SEL_{ss}$  for their vibratory pile pulses was 1 s, compared to 0.4 s in our study. The maximum sound pressure

level (zero-to-peak) and the number of piling events were 153.1 dB (re 1  $\mu\text{Pa}$ ) and 125, respectively, in their study, compared to 195.1 dB (re 1  $\mu\text{Pa}$ ) and 636 in our study. This resulted in a higher  $SEL_{w,cum}$  and a longer impact range in our study. Both studies lacked behavioral evidence to examine an animal's acute responses to pile-driving events. Future investigations should combine field experiments, model estimations, and behavioral observations to comprehensively assess pile-driving impacts and provide references for management.

Acoustic monitoring is a promising tool for effectively assessing local biodiversity in wind operation areas during different phases (Pijanowski et al., 2011; Mooney et al., 2020a, 2020b). Both biological sounds (an indicator of biodiversity) and anthropogenic sounds, including wind farm noise, are major components of the overall soundscape (Krause, 2008; Sueur and Farina, 2015). If wind farm noise disrupts animal behavior or displaces sound-producing animals, it will directly alter the biological proportion of the soundscape while increasing anthropogenic input. The characteristics of signals produced by animals and wind farm noise may vary in frequency, bandwidth, duration, and repetition rate, showing distinct properties in time and frequency domains. Therefore, long-term monitoring of the soundscape, particularly comparing soundscapes across different phases of wind farm development, is likely to reflect changes and inform policies to better manage wind farm development.

The acoustic abundance in the PRE wind farm should be carefully monitored, especially over the long term, to better understand the pros and cons and to develop strategies that balance local power input with minimizing impacts on aquatic taxa. The coming years will see the extension of wind farm construction into the western PRE, an area with high biodiversity (Wang et al., 2017, 2022; Zhang et al., 2017; Song et al., 2023b), making it urgent to evaluate the influence of wind farm noise. There are still knowledge gaps to fill concerning bioacoustics in the PRE and other areas where wind farms are or will be located. The two PRE wind farms mentioned in this study are expected to provide 1.5 GW of electricity when operational, a small portion of the total 66.9 GW planned by Guangdong Province (Deng et al., 2022; Guangdong Provincial Development and Reform Commission, 2018).

In China, offshore wind farms will play a vital role in replacing traditional energy sources (Zheng et al., 2016; Zhang et al., 2020). This study offers several key recommendations for policymakers. First, acoustic monitoring is essential for tracking biodiversity during different phases of wind farm construction. Second, the impact zone can be better estimated by collecting data on animal vocalization, distribution, and sensitivity. A combination of acoustic measurements, hearing examination, and modeling will help establish safe zones for animals during the construction phase. Finally, collaboration between scientists and government agencies is crucial for developing long-term plans.

## 5. Conclusions

The connection between anthropogenic activities and animal behavior is crucial for managing ocean-based economic activities. This research documented signals from fishes and Indo-Pacific humpback dolphins in the Pearl River Estuary (PRE) and analyzed the spectral and temporal properties of wind farm noise. During the construction phase, pile-driving events generated significantly stronger pulses compared to the normal operation phase, surpassing the vocalization and hearing thresholds of animals within 30 m of the turbine. These baseline data supported the development of a propagation model that predicted the impact zones of pile-driving noise on local animals in the PRE. The pile-driving pulses were found to have a maximum impact range of 12.8 m for fish, a temporary threshold shift zone of 580.9 m, and a permanent threshold shift zone of 32.4 m for Indo-Pacific humpback dolphins. We recommend establishing long-term acoustic monitoring stations to continuously assess the soundscape within the wind farm and to develop mitigation methods to protect the local wildlife. Implementing these measures will enable the formulation of effective management policies that allow for the construction of



wind farms with minimal impact on animals.

### CRedit authorship contribution statement

**Zhongchang Song:** conceptualization, writing – original draft, writing - review & editing, methodology, validation, funding acquisition. **Weijie Fu:** investigation, writing – original draft, writing - review & editing, data curation, methodology, formal analysis, software. **Hongquan Li:** writing - review & editing, data curation, formal analysis. **Yingnan Su:** data curation, formal analysis. **Zhanyuan Gao:** field work, formal analysis, investigation. **Wenxin Fan:** field work, data examination. **Jiangang Hui:** data curation, formal analysis. **Wenzhan Ou:** data curation, formal analysis. **Shengyao Sun:** field experiment. **Teng Wang:** field work, resources. **Honghui Huang:** funding acquisition, project administration, writing - review & editing, supervision. **Yu Zhang:** funding acquisition, project administration, writing - review & editing, validation, supervision.

### Funding

This work was funded by the National Natural Science Foundation of China [Grant Nos. 42106181; 12074323; 62231011]; the Fundamental Research Funds for the Central Universities [No.20720240106]; the Natural Science Foundation of Fujian Province of China [Nos.2024J01019; 2022J02003]; and the Development of a novel high-performance platform for deep-sea fish farming and research of its key performances for Science and Technology Major Project of Fujian Province [Grant Nos. 2021NZ033016]. The fieldwork in the wind farm region was financially supported by the Central Public-interest Scientific Institution Basal Research Fund, CAFS [NO.2023TD15]; the Special Project for Economic Development of Guangdong [GDNRC[2020]19]; the Guangzhou Science and Technology Foundation [202102020901]; and the Financial Fund of the Ministry of Agriculture and Rural Affairs, P.R. China [NO. NFXZ2021].

### Declaration of competing interest

The authors declare that they have no competing interests or personal relationships that could have appeared to influence the work reported in this paper.

### Acknowledgments

We would like to acknowledge Shaochuan Lin, Zhen Xiao, and Xiaohui Xu from the College of Ocean and Earth Sciences at Xiamen University for their help in conducting fieldwork.

### References

Accomando, A.W., Mulsow, J., Branstetter, B.K., Schlundt, C.E., Finneran, J.J., 2020. Directional hearing sensitivity for 2–30 kHz sounds in the bottlenose dolphin (*Tursiops truncatus*). *J. Acoustic. Soc. Am.* 147, 388–398. <https://doi.org/10.1121/10.0000557>.

Arneth, A., Shin, Y.J., Leadley, P., Rondinini, C., Bukvareva, E., Kolb, M., Midgley, G.F., et al., 2020. Post-2020 biodiversity targets need to embrace climate change. *P. Natl. A. Sci.* 117, 30882–30891. <https://doi.org/10.1073/pnas.2009584117>.

Bailey, H., Senior, B., Simmons, D., Rusin, J., Picken, G., Thompson, P.M., 2010. Assessing underwater noise levels during pile-driving at an offshore windfarm and its potential effects on marine mammals. *Mar. Pollut. Bull.* 60, 888–897. <https://doi.org/10.1016/j.marpolbul.2010.01.003>.

Bailey, H., Brookes, K.L., Thompson, P.M., 2014. Assessing environmental impacts of offshore wind farms: lessons learned and recommendations for the future. *Aquat. Biosyst.* 10, 1–13. <https://doi.org/10.1186/2046-9063-10-8>.

Branstetter, B.K., Bowman, V.F., Houser, D.S., Tormey, M., Banks, P., Finneran, J.J., Jenkins, K., 2018. Effects of vibratory pile driver noise on echolocation and vigilance in bottlenose dolphins (*Tursiops truncatus*). *J. Acoustic. Soc. Am.* 143, 429–439. <https://doi.org/10.1121/1.5021555>.

Breton, S.P., Moe, G., 2009. Status, plans and technologies for offshore wind turbines in Europe and North America. *Renew. Energy.* 34, 646–654.

Burrows, M.T., Schoeman, D.S., Buckley, L.B., Moore, P., Poloczanska, E.S., Brander, K.M., Brown, C., et al., 2011. The pace of shifting climate in marine and

terrestrial ecosystems. *Science* 334, 652–655. <https://doi.org/10.1016/j.renene.2008.05.040>.

Carstensen, J., Henriksen, O., Teilmann, J., 2006. Impacts of offshore wind farm construction on harbour porpoises: acoustic monitoring of echolocation activity using porpoise detectors (T-PODs). *Mar. Ecol. Prog. Ser.* 321, 295–308. <https://doi.org/10.3354/meps321295>.

Causon, P.D., Gill, A.B., 2018. Linking ecosystem services with epibenthic biodiversity change following installation of offshore wind farms. *Environ. Sci. Policy.* 89, 340–347. <https://doi.org/10.1016/j.envsci.2018.08.013>.

Cheang, C., Lee, B., Ip, B.H., Yiu, W., Tsang, L., Ang, P.O., 2020. Fish and crustacean biodiversity in an outer maritime estuary of the Pearl River Delta revealed by environmental DNA. *Mar. Pollut. Bull.* 161, 111707. <https://doi.org/10.1016/j.marpolbul.2020.111707>.

Cones, S.F., Jézéquel, Y., Ferguson, S., Aoki, N., Mooney, T.A., 2022. Pile driving noise induces transient gait disruptions in the longfin squid (*Doryteuthis pealeii*). *Front. Mar. Sci.* 9, 1–13. <https://doi.org/10.3389/fmars.2022.1070290>.

Cook, A.S.C.P., Humphreys, E.M., Bennet, F., Masden, E.A., Burton, N.H.K., 2018. Quantifying avian avoidance of offshore wind turbines: current evidence and key knowledge gaps. *Mar. Environ. Res.* 140, 278–288. <https://doi.org/10.1016/j.marenvres.2018.06.017>.

Corbetta, G., Pineda, I., Moccia, J., 2014. The European Offshore Wind Industry - Key Trends and Statistics 2013. European Wind Energy Association (EWEA). Report by.

Davidson, J.G., Dong, H., Linné, M., Andersson, M.H., Piper, A., Prystay, T.S., Hvam, E.B., et al., 2019. Effects of sound exposure from a seismic airgun on heart rate, acceleration and depth use in free-swimming Atlantic cod and saithe. *Conserv. Physiol.* 7, coz020. <https://doi.org/10.1093/conphys/coz020>.

Debusschere, E., De Coensel, B., Vandendriessche, S., Botteldooren, D., Hostens, K., Vincx, M., Degraer, S., 2016. Effects of offshore wind farms on the early life stages of *Dicentrarchus labrax*. In: Popper, A.N., Hawkins, A. (Eds.), *The Effects of Noise on Aquatic Life II*. Springer, New York, New York, America, pp. 197–204.

Deng, X., Xu, W., Xu, Y., Shao, Y., Wu, X., Yuan, W., Qin, Z., 2022. Offshore wind power in China: a potential solution to electricity transformation and carbon neutrality. *Fundamental Research.* <https://doi.org/10.1016/j.fmre.2022.11.008>.

de Jong, K., Forland, T.N., Amorim, M.C.P., Rieucou, G., Slabbekoorn, H., Sivle, L.D., 2020. Predicting the effects of anthropogenic noise on fish reproduction. *Rev. Fish. Biol. Fisher.* 30, 245–268. <https://doi.org/10.1007/s11160-020-09598-9>.

Dinh, J.P., Radford, C., 2021. Acoustic particle motion detection in the snapping shrimp (*Alpheus richardsoni*). *J. Comp. Physiol. A.* 207, 641–655. <https://doi.org/10.1007/s00359-021-01503-4>.

Doney, S.C., Ruckelshaus, M., Emmett Duffy, J., Barry, J.P., Chan, F., English, C.A., Galindo, H.M., et al., 2012. Climate change impacts on marine ecosystems. *Annu. Rev. Mar. Sci.* 4, 11–37.

Elmer, K.H., 2018. Effective offshore piling noise mitigation in deep waters. *Journal of Civil Engineering and Architecture* 12, 662–668. <https://doi.org/10.17265/1934-7359/2018.09.006>.

Ellison, W.T., Southall, B.L., Clark, C.W., Frankel, A.S., 2012. A New context-based approach to assess marine mammal behavioral responses to anthropogenic sounds. *Conserv. Biol.* 26, 21–28. <https://doi.org/10.1111/j.1523-1739.2011.01803.x>.

Furness, R.W., Wade, H.M., Robbins, A.M.C., Masden, E.A., 2012. Assessing the sensitivity of seabird populations to adverse effects from tidal stream turbines and wave energy devices. *ICES J. Mar. Sci.* 69, 1466–1479. <https://doi.org/10.1093/icesjms/fss131>.

Gielen, D., Boshell, F., Saygin, D., Bazilian, M.D., Wagner, N., Gorini, R., 2019. The role of renewable energy in the global energy transformation. *Energy Strateg. Rev.* 24, 38–50. <https://doi.org/10.1016/j.esr.2019.01.006>.

Global wind energy council, 2020. *Global Offshore Wind Report 2020*.

Guangdong Provincial Development and Reform Commission, 2018. Development planning of offshore wind power in Guangdong, Province. Available online: [http://drc.gd.gov.cn/gkmlpt/content/1/1060/post\\_1060661.html#876](http://drc.gd.gov.cn/gkmlpt/content/1/1060/post_1060661.html#876).

Hall, R., João, E., Knapp, C.W., 2020. Environmental impacts of decommissioning: onshore versus offshore wind farms. *Environ. Impact Asses.* 83, 106404. <https://doi.org/10.1016/j.eiar.2020.106404>.

Halvorsen, M.B., Casper, B.M., Woodley, C.M., Carlson, T.J., Popper, A.N., 2011. Predicting and mitigating hydroacoustic impacts on fish from pile installation. NCHRP Report Research Results Digest 363, Project 25-28. National Cooperative Highway Research Program, Transportation Research Board. National Academy of Sciences, Washington, D.C.

Halvorsen, M.B., Casper, B.M., Woodley, C.M., Carlson, T.J., Popper, A.N., 2012. Threshold for onset of injury in Chinook salmon from exposure to impulsive pile driving sounds. *PLoS One* 7 (6), e38968. <https://doi.org/10.1371/journal.pone.0038968>.

Han, D.G., Choi, J.W., 2022. Measurements and spatial distribution simulation of impact pile driving underwater noise generated during the construction of offshore wind power plant off the southwest coast of Korea. *Front. Mar. Sci.* 8, 654991. <https://doi.org/10.3389/fmars.2021.654991>.

Hawkins, A.D., Popper, A.N., 2017. A sound approach to assessing the impact of underwater noise on marine fishes and invertebrates. *ICES J. Mar. Sci.* 74, 635–651. <https://doi.org/10.1093/icesjms/fsw205>.

Hoegh-Guldberg, O., Jacob, D., Taylor, M., Guillén Bolaños, T., Bindi, M., Brown, S., Camilloni, I.A., et al., 2019. The human imperative of stabilizing global climate change at 1.5°C. *Science.* 365, eaaw6974. <https://doi.org/10.1126/science.aaw6974>.

Horodysky, A.Z., Brill, R.W., Fine, M.L., Musick, J.A., Latour, R.J., 2008. Acoustic pressure and particle motion thresholds in six sciaenid fishes. *J. Exp. Biol.* 211 (9), 1504–1511. <https://doi.org/10.1242/jeb.016196>.

- Huang, H., Lin, Y., Li, C., Lin, Q., Cai, W., Gao, D., Jia, X., 2002. Ecology study on the benthic animals of Pearl River Estuary. *Acta Ecol. Sin.* 22, 603–607. <https://doi.org/10.3321/j.issn:1000-0933.2002.04.024>.
- Huang, S.L., Karczmarski, L., Chen, J., Zhou, R., Lin, W., Zhang, H., Li, H., et al., 2012. Demography and population trends of the largest population of Indo-Pacific humpback dolphins. *Biol. Conserv.* 147, 234–242. <https://doi.org/10.1016/j.biocon.2012.01.004>.
- Hughes, A.R., Mann, D.A., Kimbro, D.L., 2014. Predatory fish sounds can alter crab foraging behaviour and influence bivalve abundance. *P. Roy. Soc. B-Biol. Sci.* 281, 20140715. <https://doi.org/10.1098/rspb.2014.0715>.
- IRENA, 2020. Global renewables outlook. Energy Transformation 2050, Edition: 2020. International Renewable Energy Agency, Abu Dhabi.
- Jézéquel, Y., Jones, I.T., Bonnel, J., Chauvaud, L., Atema, J., Mooney, T.A., 2021. Sound detection by the American lobster (*Homarus americanus*). *J. Exp. Biol.* 224, jeb240747. <https://doi.org/10.1242/jeb.240747>.
- Jones, I.T., Peyla, J.F., Clark, H., Song, Z., Stanley, J.A., Mooney, T.A., 2021. Changes in feeding behavior of longfin squid (*Doryteuthis pealeii*) during laboratory exposure to pile driving noise. *Mar. Environ. Res.* 165, 105250. <https://doi.org/10.1016/j.marenvres.2020.105250>.
- Koschinski, S., Culik, B., Damsgaard Henriksen, O., Tregenza, N., Ellis, G., Jansen, C., Kathe, G., 2003. Behavioural reactions of free-ranging porpoises and seals to the noise of a simulated 2 MW windpower generator. *Mar. Ecol. Prog. Ser.* 265, 263–273. <https://doi.org/10.3354/meps265263>.
- Koschinski, S., Lüdemann, K., 2020. Noise mitigation for the construction of increasingly large offshore wind turbines. Report for German Federal Agency for Nature Conservation (BfN).
- Krause, B., 2008. Anatomy of the soundscape evolving perspectives. *J. Audio Eng. Soc.* 56, 73–80.
- Kuang, T., Chen, W., Huang, S., Liu, L., Zhou, L., 2021. Environmental drivers of 2007. An acoustical hypothesis for the spiral bubble nets of humpback whales and the impth functional structure of fish communities in the Pearl River Estuary. *Estuar. Coast. Shelf S.* 263, 107625. <https://doi.org/10.1016/j.ecss.2021.107625>.
- Ladich, F., Fay, R.R., 2013. Auditory evoked potential audiometry in fish. *Rev. Fish Biol. Fish.* 23, 317–364. <https://doi.org/10.1007/s11160-012-9297-z>.
- Langhamer, O., Dahlgren, T.G., Rosenqvist, G., 2018. Effect of an offshore wind farm on the viviparous eelpout: biometrics, brood development and population studies in Lillgrund, Sweden. *Ecol. Indic.* 84, 1–6. <https://doi.org/10.1016/j.ecolind.2017.08.035>.
- Leunissen, E.M., Rayment, W.J., Dawson, S.M., 2019. Impact of pile-driving on Hector's dolphin in Lyttelton harbour, New Zealand. *Mar. Pollut. Bull.* 142, 31–42. <https://doi.org/10.1016/j.marpolbul.2019.03.017>.
- Li, H., Song, Z., Hui, J., Su, Y., Fu, W., Zhang, S., Yan, L., et al., 2023. Vocalization behavior of Chinese bahaba (*Bahaba taipingensis*) during the reproduction season. *J. Mar. Sci. Eng.* 11, 712. <https://doi.org/10.3390/jmse11040712>.
- Li, S., Wang, D., Wang, K., Taylor, E.A., Cros, E., Shi, W., Wang, Z., et al., 2012. Evoked potential audiogram of an Indo-Pacific humpback dolphin (*Sousa chinensis*). *J. Exp. Biol.* 070904. <https://doi.org/10.1242/jeb.070904>.
- Lian, J., Hou, G., Cai, O., Xu, K., 2022. Assessing the life cycle risks of offshore wind turbines with suction bucket foundations. *J. Clean. Prod.* 362, 132366. <https://doi.org/10.1016/j.jclepro.2022.132366>.
- Lucke, K., Lepper, P.A., Blanchet, M.A., Siebert, U., 2011. The use of an air bubble curtain to reduce the received sound levels for harbor porpoises (*Phocoena phocoena*). *J. Acoustic. Soc. Am.* 130, 3406–3412. <https://doi.org/10.1121/1.3626123>.
- Martin, S.B., Morris, C., Bröker, K., O'Neill, C., 2019. Sound exposure level as a metric for analyzing and managing underwater soundscapes. *J. Acoustic. Soc. Am.* 146, 135–149. <https://doi.org/10.1121/1.5113578>.
- Mooney, T.A., Hanlon, R.T., Christensen-Dalsgaard, J., Madsen, P.T., Ketten, D.R., Nachtigall, P.E., 2010. Sound detection by the longfin squid (*Loligo pealeii*) studied with auditory evoked potentials: sensitivity to low-frequency particle motion and not pressure. *J. Exp. Biol.* 213, 3748–3759. <https://doi.org/10.1242/jeb.048348>.
- Mooney, T.A., Andersson, M., Stanley, J., 2020a. Acoustic impacts of offshore wind energy on fishery resources: an evolving source and varied effects across a wind farm's lifetime. *Oceanography* 33, 82–95. <https://doi.org/10.5670/oceanog.2020.408>.
- Mooney, T.A., Iorio, L.D., Lammers, M., Lin, T.H., Nedelec, S.L., Parsons, M., Radford, C., et al., 2020b. Listening forward: approaching marine biodiversity assessments using acoustic methods. *Roy. Soc. Open Sci.* 7, 201287. <https://doi.org/10.1098/rsos.201287>.
- Nachtigall, P.E., Supin, A.Y., 2008. A false killer whale adjusts its hearing when it echolocates. *J. Exp. Biol.* 211, 1714–1718. <https://doi.org/10.1242/jeb.013862>.
- National Marine Fisheries Service, 2018. 2018 Revisions to: Technical Guidance for Assessing the Effects of Anthropogenic Sound on Marine Mammal Hearing (Version 2.0): Underwater Thresholds for Onset of Permanent and Temporary Threshold Shifts. U.S. Department of Commerce, NOAA, p. 167. NOAA Technical Memorandum NMFS-OPR-59.
- Neo, Y.Y., Hubert, J., Bolle, L., Winter, H.V., Ten Cate, C., Slabbekoorn, H., 2016. Sound exposure changes European seabass behaviour in a large outdoor floating pen: effects of temporal structure and a ramp-up procedure. *Environ. Pollut.* 214, 26–34. <https://doi.org/10.1016/j.envpol.2016.03.075>.
- Niu, F., Xie, J., Zhang, X., Xue, R., Chen, B., Liu, Z., Yang, Y., 2023. Assessing differences in acoustic characteristics from impact and vibratory pile installation and their potential effects on the large yellow croaker (*Pseudosciaena crocea*). *Front. Mar. Sci.* 10, 1106980. <https://doi.org/10.3389/fmars.2023.1106980>.
- Oliveira, T.C., Lin, Y.T., Porter, M.B., 2021. Underwater sound propagation modeling in a complex shallow water environment. *Front. Mar. Sci.* 8, 751327.
- Pijanowski, B.C., Villanueva-Rivera, L.J., Dumyahn, S.L., Farina, A., Krause, B.L., Napoletano, B.M., Gage, S.H., et al., 2011. Soundscape ecology: the science of sound in the landscape. *Bioscience* 61, 203–216. <https://doi.org/10.1525/bio.2011.61.3.6>.
- Popper, A.N., Hawkins, A.D., 2018. The importance of particle motion to fishes and invertebrates. *J. Acoust. Soc. Am.* 143 (1), 470–488. <https://doi.org/10.1121/1.5021594>.
- Popper, A.N., Hawkins, A.D., Sand, O., Sisneros, J.A., 2019. Examining the hearing abilities of fishes. *J. Acoustic. Soc. Am.* 146, 948–955. <https://doi.org/10.1121/1.5120185>.
- Popper, A.N., Hice-Dunton, L., Jenkins, E., Higgs, D.M., Krebs, J., Mooney, A., Rice, A., et al., 2022. Offshore wind energy development: research priorities for sound and vibration effects on fishes and aquatic invertebrates. *J. Acoustic. Soc. Am.* 151, 205–215. <https://doi.org/10.1121/10.0009237>.
- Reinhall, P.G., Dahl, P.H., 2011. Underwater Mach wave radiation from impact pile driving: theory and observation. *J. Acoustic. Soc. Am.* 130, 1209–1216. <https://doi.org/10.1121/1.3614540>.
- Salas, A.K., Ballard, M.S., Mooney, T.A., Wilson, P.S., 2022. Effects of frequency-dependent spatial variation in soundscape settlement cues for reef fish larvae. *Mar. Ecol. Prog. Ser.* 687, 1–21.
- Scheidat, M., Tougaard, J., Brasseur, S., Carstensen, J., van Polanen Petel, T., Teilmann, J., Reijnders, P., 2011. Harbour porpoises (*Phocoena phocoena*) and wind farms: a case study in the Dutch North Sea. *Environ. Res. Lett.* 6, 025102. <https://doi.org/10.1088/1748-9326/6/2/025102>.
- Siddagangaiah, S., Chen, C.F., Hu, W.C., Pieretti, N., 2022. Impact of pile-driving and offshore windfarm operational noise on fish chorusing. *Remote Sens. Ecol. Con.* 8, 119–134. <https://doi.org/10.1002/rse2.231>.
- Sigray, P., Linné, M., Andersson, M.H., Nöjd, A., Persson, L.K.G., Gill, A.B., Thomsen, F., 2022. Particle motion observed during offshore wind turbine piling operation. *Mar. Pollut. Bull.* 180, 113734. <https://doi.org/10.1016/j.marpolbul.2022.113734>.
- Song, Z., Mooney, T.A., Quakenbush, L., Hobbs, R., Gaglione, E., Goertz, C., Castellote, M., 2023a. Variability of echolocation clicks in beluga whales (*Delphinapterus leucas*) within shallow waters. *Aquat. Mamm.* 49, 62–72. <https://doi.org/10.1578/am.49.1.2023.62>.
- Song, Z., Ou, W., Su, Y., Li, H., Fan, W., Sun, S., Wang, T., et al., 2023b. Sounds of snapping shrimp (*Alpheidae*) as important input to the soundscape in the southeast China coastal sea. *Front. Mar. Sci.* 10, 1029003. <https://doi.org/10.3389/fmars.2023.1029003>.
- Song, Z., Li, H., Su, Y., Cao, P., Ou, W., Sun, S., Fu, W., et al., 2023c. Investigation on pile driving noise production and mitigation through bubble curtain. In: Yang, D. (Ed.), International Conference on Marine Equipment & Technology and Sustainable Development. Springer Nature Singapore, Singapore, pp. 1–9. [https://doi.org/10.1007/978-981-99-4291-6\\_1](https://doi.org/10.1007/978-981-99-4291-6_1), 2023c.
- Southall, B.L., Bowles, A.E., Ellison, W.T., Finneran, J.J., Gentry, R.L., Greene, C.R., Kastak, D., et al., 2008. Marine mammal noise exposure criteria: initial scientific recommendations. *Bioacoustics* 17, 273–275. <https://doi.org/10.1080/09524622.2008.9753846>.
- Southall, B.L., Finneran, J.J., Reichmuth, C., Nachtigall, P.E., Ketten, D.R., Bowles, A.E., Ellison, W.T., et al., 2019. Marine mammal noise exposure criteria: updated scientific recommendations for residual hearing effects. *Aquat. Mamm.* 45, 125–232. <https://doi.org/10.1578/am.45.2.2019.125>.
- Stanley, J.A., Van Parijs, S.M., Hatch, L.T., 2017. Underwater sound from vessel traffic reduces the effective communication range in Atlantic cod and haddock. *Sci. Rep-UK* 7, 14633. <https://doi.org/10.1038/s41598-017-14743-9>.
- Sueur, J., Farina, A., 2015. Ecoacoustics: the ecological investigation and interpretation of environmental sound. *Biosemiotics* 8, 493–502. <https://doi.org/10.1007/s12304-015-9248-x>.
- Tougaard, J., Carstensen, J., Teilmann, J., Skov, H., Rasmussen, P., 2009. Pile driving zone of responsiveness extends beyond 20 km for harbor porpoises (*Phocoena phocoena* (L.)). *J. Acoustic. Soc. Am.* 126, 11–14. <https://doi.org/10.1121/1.3132523>.
- Tougaard, J., Beedholm, K., 2019. Practical implementation of auditory time and frequency weighting in marine bioacoustics. *Appl. Acoust.* 145, 137–143. <https://doi.org/10.1016/j.apacoust.2018.09.022>.
- Tougaard, J., Hermanssen, L., Madsen, P.T., 2020. How loud is the underwater noise from operating offshore wind turbines? *J. Acoustic. Soc. Am.* 148, 2885–2893. <https://doi.org/10.1121/10.0002453>.
- Tu, Q., Liu, Z., Li, B., Mo, J., 2021. Achieving grid parity of offshore wind power in China—A comparative analysis among different provinces. *Comput. Ind. Eng.* 162, 107715. <https://doi.org/10.1016/j.cie.2021.107715>.
- Umar, H.A., Sulaiman, S.A., Meor Said, M.A., Gungor, A., Shahbaz, M., Inayat, M., Ahmad, R.K., 2021. Assessing the implementation levels of oil palm waste conversion methods in Malaysia and the challenges of commercialisation: towards sustainable energy production. *Biomass Bioenergy* 151, 106179. <https://doi.org/10.1016/j.biombioe.2021.106179>.
- U.S. Energy Information Administration, 2019. Electric power sector CO<sub>2</sub> emissions drop as generation mix shifts from coal to natural gas. Washington, DC. Available online: <https://www.eia.gov/todayinenergy/detail.php?id=equals;48296>.
- Vanermen, N., Onkelinx, T., Courtens, W., Van de walle, M., Verstraete, H., Stienen, E.W.M., 2015. Seabird avoidance and attraction at an offshore wind farm in the Belgian part of the North Sea. *Hydrobiologia* 756, 51–61. <https://doi.org/10.1007/s10750-014-2088-x>.
- Wang, Z., Wu, Y., Duan, G., Cao, H., Liu, J., Wang, K., Wang, D., 2014. Assessing the underwater acoustics of the world's largest vibration hammer (OCTA-KONG) and its potential effects on the indo-pacific humpbacked dolphin (*Sousa chinensis*). *PLoS One* 9, e110590. <https://doi.org/10.1371/journal.pone.0110590>.

- Wang, Z., Nowacek, D.P., Akamatsu, T., Wang, K., Liu, J., Duan, G., Cao, H., et al., 2017. Diversity of fish sound types in the Pearl River Estuary, China. *PeerJ* 5, e3924. <https://doi.org/10.7287/peerj.preprints.3301v1>.
- Wang, T., Zhang, P., Zhang, S., Liu, Q., Liao, X., Rao, Y., Huang, H., et al., 2022. Acoustic assessment of fishery resources in jinwan offshore wind farm area. *J. Mar. Sci. Eng.* 10, 1938. <https://doi.org/10.3390/jmse10121938>.
- Wilhelmsson, D., Malm, T., Öhman, M.C., 2006. The influence of offshore windpower on demersal fish. *ICES J. Mar. Sci.* 63, 775–784. <https://doi.org/10.1016/j.icesjms.2006.02.001>.
- Wilson, J.C., Elliott, M., Cutts, N.D., Mander, L., Mendão, V., Perez-Dominguez, R., Phelps, A., 2010. Coastal and offshore wind energy generation: is it environmentally benign? *Energies* 3, 1383–1422. <https://doi.org/10.3390/en3071383>.
- Xie, J., Xue, R., Niu, F., Chen, B., Yang, Y., 2024. Three-dimensional acoustic propagation of noise from impact pile driving in a complex costal environment and its effects on large yellow croaker (*Pseudosciaena crocea*). *Front. Mar. Sci.* 11, 1395120. <https://doi.org/10.3389/fmars.2024.1395120>.
- Yang, W., Luo, W., Zhang, Y., 2017. Automatic detection method for monitoring odontocete echolocation clicks. *Electron. Lett.* 53, 367–368. <https://doi.org/10.1049/el.2016.4590>.
- Zhang, S., Wei, J., Chen, X., Zhao, Y., 2020. China in global wind power development: role, status and impact. *Renew. Sust. Energ. Rev.* 127, 109881. <https://doi.org/10.1016/j.rser.2020.109881>.
- Zhang, X., Lin, W., Yu, R.-Q., Sun, X., Ding, Y., Chen, H., Chen, X., et al., 2017. Tissue partition and risk assessments of trace elements in indo-pacific finless porpoises (*Neophocaena phocaenoides*) from the Pearl River Estuary coast, China. *Chemosphere* 185, 1197–1207. <https://doi.org/10.1016/j.chemosphere.2017.07.080>.
- Zhang, X., Guo, H., Chen, J., Song, J., Xu, K., Lin, J., Zhang, S., 2021. Potential effects of underwater noise from wind turbines on the marbled rockfish (*Sebasticus marmoratus*). *J. Appl. Ichthyol.* 37, 514–522. <https://doi.org/10.1111/jai.14198>.
- Zhang, C., Wu, F.X., Song, Z.C., Fu, W.J., Xiang, W.J., Ou, W.Z., Zhang, Y., 2024. Exploring the time-varying directivity of whistles in the Indo-Pacific humpback dolphin (*Sousa chinensis*). In: *In Revision*.
- Zheng, C., Li, C., Pan, J., Liu, M., Xia, L., 2016. An overview of global ocean wind energy resource evaluations. *Renew. Sust. Energ. Rev.* 53, 1240–1251. <https://doi.org/10.1016/j.rser.2015.09.063>.
- Zhou, M., Zhang, H., Lv, T., Li, H., Xiang, D., Huang, S., Gulliver, T.A., 2022. Underwater acoustic channel modeling under different shallow seabed topography and sediment environment. In: *OCEANS 2022-Chennai*. IEEE, pp. 1–7.